

Hydrogen-bonding modulation of excited-state properties of flavins in a model of aqueous confined environment†‡

Lorena Valle, Faustino E. Morán Vieyra and Claudio D. Borsarelli*

Received 19th November 2011, Accepted 5th March 2012

DOI: 10.1039/c2pp05385c

The singlet and triplet excited states properties of lumiflavin (LF), riboflavin (RF), flavin mononucleotide (FMN) and flavin adenine dinucleotide (FAD) in reversed micelles (RM) of sodium docusate (AOT) in n-hexane solutions were evaluated as a function of the water to surfactant molar ratio, $w_0 = [\text{H}_2\text{O}]/[\text{AOT}]$, by both steady-state and time-resolved absorption and fluorescence spectroscopy. The results indicated that hydrogen-bonding interactions between the isoalloxazine ring of the flavins with the water molecules of the micellar interior play a crucial role on the modulation of the excited state properties of the flavins. Fluorescence dynamic experiments in the RM, allowed the calculation of similar values for both the internal rotational time of the flavins (θ_i) and the hydrogen-bonding relaxation time (τ_{HB}), *e.g.* ≈ 7 and 1.5 ns at $w_0 = 1$ and 20, respectively. In turn, the triplet state lifetimes of the flavins were also enlarged in RM solutions at low w_0 , without modifications of their quantum yields. A hydrogen bonding relaxation model is proposed to explain the singlet excited state properties of the flavins, while the changes of the triplet state decays of the flavins were related with the global composition and strength of the hydrogen bonding network inside of the RM.

Introduction

Flavins belong to a huge family of bioactive compounds found in redox enzymes and photoreceptors, with flavin mononucleotide (FMN) and flavin adenine dinucleotide (FAD) as ubiquitous cofactors.^{1,2} Riboflavin (RF) is one of the components of the B₂ vitamin complex, and is essential in living organisms. Furthermore, RF is present in several foods and beverages, such as dairy products, beer, beans, *etc.*, where can it act as a photosensitizer.³ In anaerobic conditions, UVA-Vis photolysis of RF yields lumiflavin (LF) as main photoproduct.⁴ All these flavins have the same oxidized isoalloxazine ring as chromophore and/or redox mediator, and in the case of RF, FMN and FAD share a ribityl side chain that plays chemical and biological roles.⁵ Therefore, the spectroscopic and photochemical properties of both isoalloxazine ring and flavin derivatives either in homogeneous solutions or in protein environments have been a matter of current interest in recent decades.^{6–12} Despite the importance of flavins as cofactors in enzymes, where the active sites are highly organized, there are few reports on the spectroscopic and

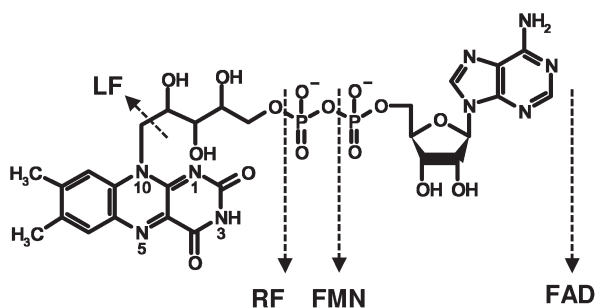
photophysical properties of flavins in organized or constrained artificial media.^{13–16}

In this sense, the reversed micelles (RM) are appropriate candidates for such studies because their environmental properties can be well controlled by changing the proportion of water entrapped in the microemulsion. The physical and chemical properties of water inside of RM are markedly different from the properties of bulk water but similar in several aspects to those of biological interfacial water as found in membrane or protein interfaces.¹⁷ The highly structured, yet heterogeneous water molecules in RM simulates adequately water molecules present in biological systems such as membranes, which are difficult to analyze experimentally. Basically, RM are spherical self-assembly structures dispersed in an organic solvent (oil), consisting of a surfactant monolayer that encapsulates water droplets of nanoscopic size (approximately between 1–20 nm in diameter).^{18,19} The RM solutions are thermodynamically stable and optically transparent in a wide range of water and surfactant concentrations. Typically, the properties of the RM depend on its size, which is proportional to the water to surfactant molar ratio, *i.e.* $w_0 = [\text{H}_2\text{O}]/[\text{Surf}]$.¹⁷ Aerosol-OT (AOT) or sodium docusate salt is the most extensively used surfactant to form RM in organic solvents, such as n-alkanes, dissolving large amount of water (*e.g.* up to $w_0 \approx 50$ –60). The structure and properties of the RM solutions formed with AOT have been extensively characterized by several methods.^{18–26} For AOT RM formed at $w_0 < 10$, it has been well established that inner water molecules are rigidly immobilized in the solvation of the anionic polar heads of AOT and sodium counterions. In this condition, the interior of RM is highly viscous and shows lower polarity than bulk water. At w_0

Laboratorio de Cinética y Fotoquímica (LACIFO), Instituto de Química del Noroeste Argentino (INQUINOA-CONICET), Universidad Nacional de Santiago del Estero (UNSE), RN 9, Km 1125, Villa El Zanjón, CP 4206 Santiago del Estero, Argentina. E-mail: cborsarelli@yahoo.com.ar; Tel: +54-385-4509528. Int. 1797

† This article is published as part of a themed issue in honour of Professor Kurt Schaffner on the occasion of his 80th birthday.

‡ Electronic supplementary information (ESI) available. See DOI: 10.1039/c2pp05385c



Scheme 1 Structure formula of the flavins: lumiflavin (LF), riboflavin (RF), flavin mononucleotide (FMN) and flavin adenine dinucleotide (FAD).

> 10, the solvation of the internal micellar interface (surfactant monolayer + solvated double electrical layer) is complete, and additional water molecules are forming a nano-sized water pool with “free” water molecules at the center of the RM. In this condition, both the micellar interface and the waterpool are less rigid, and the internal water molecules begin to have properties similar to those of pure water.^{18–26} Due to the spherical shape of the AOT RM a radial dependence of the internal environmental properties (*e.g.* viscosity, polarity, hydrogen bonding ability, *etc.*) could be expected. These facts make RM good candidates for studying the properties of the excited states of flavins in a confined aqueous environment, as was previously showed for FMN entrapped in water pools of RM of different surfactants,¹⁵ and for an amphiphilic flavin derivative anchored into the micellar interface of AOT RM.¹⁶

In this manuscript, we extended the pioneering work of Visser *et al.* for the spectroscopic and dynamic fluorescence behavior of FMN in AOT RM,¹⁵ by studying the singlet and triplet excited state properties of the four structurally related flavins LF, RF, FMN and FAD (Scheme 1) as a function of the water content (w_0) entrapped in AOT RM solutions.

The results show that there is a controlled modulation of the properties of both singlet and triplet excited states of the flavins by the amount and strength of hydrogen bonding interactions of the isoalloxazine ring with the water molecules of the micellar interior. The dynamical properties of the hydrogen-bonding relaxation around the singlet excited state of the flavins were determined as a function of w_0 by the calculation of the time-resolved area normalized emission spectra (TRANES).

Materials and methods

Materials

Lumiflavin (LF), riboflavin (RF), flavin mononucleotide (FMN), and flavin adenine dinucleotide (FAD) were purchased from Sigma-Aldrich (Argentina) in their highest purity grade (>95%), and used without further treatment. Time-resolved emission experiments (see below) of all flavins in neutral aqueous or sodium phosphate buffer solutions showed fluorescence lifetimes coincident with reported values.^{5,12,15} Furthermore, time-resolved emission spectra (TRES) in aqueous solutions confirmed the presence of a single emitting excited state without interference of impurities. Sodium docusate salt (AOT),

Na_2HPO_4 , NaH_2PO_4 , and fluorescein as sodium salt were also from Sigma-Aldrich (Argentina). Organic solvents of spectroscopic grade were from Sintorgan SRL (Bs.As. Argentina), and were previously dehydrated with 5 Å molecular sieves. Compressed ultrapure argon was purchased from Indura SRL (S.M. de Tucumán, Argentina). Water was triply distilled.

Methods

Preparation of AOT reverse micelle solutions

Reversed micelle (RM) solutions of 0.1–0.3 M sodium docusate salt (AOT) were prepared by direct dissolution of the surfactant in n-hexane using ultrasound sonication for 20 min. Flavins were incorporated into 2 mL of AOT–n-hexane solutions by adding 2–5 μL of a concentrated stock of the flavins to 10 mM sodium phosphate buffer (PB) solution at pH 7. Under this condition, the final concentration of the flavins was about 7 μM assuring a water-to-surfactant molar ratio $w_0 = [\text{H}_2\text{O}]/[\text{AOT}] < 1$. The w_0 value was increased by adding small aliquots of PB solution, without exceeding 5–7% of the initial volume. All experiments were performed at 25(\pm 1) °C.

Steady-state spectroscopic measurements

Absorption spectra were registered with a Hewlett Packard 8453 UV-visible spectrophotometer (Palo Alto, CA, USA). Corrected fluorescence emission and excitation spectra were recorded with a Hitachi F-2500 spectrofluorimeter (Kyoto, Japan) equipped with an R-928 photomultiplier, in 1.0 cm path quartz cells using excitation and emission slits of 5 nm bandwidth. Fluorescence quantum yield (Φ_F) of the flavins was determined by excitation at 450 nm using fluorescein in 0.1 N NaOH ($\Phi_F = 0.95$) as reference,²⁷ by comparing the integrated fluorescence intensity of the sample and reference solutions matched in absorbance at the excitation wavelength as described elsewhere.²⁸ Correction by the difference of the refractive index of the media was performed and the absorbance of both sample and reference solutions at 450 nm was kept ≤ 0.05 to avoid inner filter effects.

Steady-state fluorescence anisotropy $\langle r \rangle$ was determined using the classical L-format and calculated with eqn (1), where I_{VV} and I_{VH} are the fluorescence intensities with different orientation of the excitation and emission polarizers, indicating the position by the subscripts V (vertical) and H (horizontal), respectively. The G factor represents the sensitivity ratio of the detection system for vertically and horizontally polarized light calculated as I_{HV}/I_{HH} .

$$\langle r \rangle = \frac{I_{VV} - GI_{VH}}{I_{VV} + 2GI_{VH}} \quad (1)$$

Time-resolved measurements

Fluorescence and anisotropy decays were obtained with a Tempro-01 apparatus of Horiba Jobin Yvon (Glasgow, UK), using as excitation pulse source an ultrafast 340(\pm 15) nm Nanoled®, operating at 1 MHz. The emission wavelength was selected at 520 nm with a monochromator with emission

bandwidth selected at 12 nm. All measurements were performed at room temperature and under air-saturated conditions. The fluorescence intensity decay was fitted with the Fluorescence Decay Analysis Software DAS6® of Horiba Jobin Yvon by deconvolution of the pulse function using the multi-exponential model function eqn (2),

$$I(t) = \sum_{i=1}^n \alpha_i \exp(-t/\tau_i) \quad (2)$$

where n is the number of single exponential decays, τ_i and α_i are the decay time and the fluorescence intensity amplitude at $t = 0$ of each decay, respectively. In the case of $n > 1$, the average lifetime ($\langle \tau \rangle$) was calculated with eqn (3), where f_i is the fractional contribution of each decay time to the steady-state intensity.

$$\langle \tau \rangle = \sum_{i=1}^n f_i \tau_i = \frac{\sum_{i=1}^n \alpha_i \tau_i^2}{\sum_{i=1}^n \alpha_i \tau_i} \quad (3)$$

Time-resolved decay of fluorescence anisotropy $r(t)$ was analyzed with the classical exponential model function for a spherical molecule, eqn (4),²⁸ where r_0 is the anisotropy at $t = 0$, and θ is the rotational correlation time of the sphere.

$$r(t) = r_0 \exp(-t/\theta) \quad (4)$$

Time-resolved emission spectra (TRES) corrected by the quantum efficiency of the photomultiplier response were obtained by collecting counts for 200 s for each decay time. The spectra were recorded between 450–650 nm with wavelength steps of 5 nm. The slices of TRES ($I(\lambda, t)$) at different times were constructed from the deconvoluted decay function using the global exponential fitting routine of the DAS6® software to obtain the wavelength-dependent pre-exponential factor $\alpha_i(\lambda)$ associated with τ_i decay time. This procedure minimizes the noise contribution in the TRES at the end of the decay time.

In turn, the emission spectrum associated with each decay component, $I_i(\lambda)$, or decay associated spectrum (DAS), was calculated by the product of steady-state emission spectrum $I_{ss}(\lambda)$ with the fractional contribution of each decay time at each emission wavelength, $f_i(\lambda)$, using the $\alpha_i(\lambda)$ and τ_i from the global exponential fitting analysis routine, eqn (5).

$$I_i(\lambda) = f_i(\lambda) I_{ss}(\lambda) = \frac{\alpha_i(\lambda) \tau_i}{\sum_i \alpha_i(\lambda) \tau_i} I_{ss}(\lambda) \quad (5)$$

Time-resolved area normalized emission spectroscopy (TRANES), $I_N(\lambda, t)$, were obtained by area normalization of each TRES ($I(\lambda, t)$), to match the spectral area at time t with that of $t = 0$, according to the method proposed by Koti *et al.*²⁹

$$I_N(\lambda, t) = \frac{\int I_0(\lambda) d\lambda}{\int I_t(\lambda) d\lambda} I(\lambda, t) \quad (6)$$

Laser flash photolysis (LFP) experiments were performed by excitation with the third harmonic at 355 nm of a Nd:YAG Mini-lite II laser (7 ns FWHM) (Continuum Inc, Santa Clara, CA, USA). The transient absorption spectra of Ar-saturated solutions of flavins ($\approx 50 \mu\text{M}$) were recorded with the m-LFP 112 laser-flash photolysis apparatus (Luzchem, Canada) linked to a

300 MHz Tektronik TDS 3032B digital oscilloscope for signal acquisition. The signal analysis was done with the OriginPro 8.0 software from OriginLab Corporation (USA). Triplet quantum yield (Φ_T) determinations of the flavins were done by monitoring the initial transient absorbance change at 710 nm (ΔA_{0710}) as a function of the absorbed excitation energy [$E_a = (1 - 10^{-A_{355}}) E_{355}$]. The amount of incident laser energy E_{355} , was controlled using a set of $\text{Na}_2\text{Cr}_2\text{O}_7$ solutions of 10–90% T at 355 nm, and measured with a pyroelectric powermeter Melles-Griot model 13PEM001 (USA). The Φ_T value of the flavins in AOT solutions was obtained by comparison of the linear slopes of (ΔA_{0710}) vs. E_a , using the signal of RF or FMN in PB as reference ($\Phi_T = 0.60$).³⁰ In all cases, good linear plots ($n = 6$, $r > 0.985$) with zero intercepts were obtained. Independently of the flavin derivative, the same extinction coefficient ($\epsilon_{710} = 4200 \text{ M}^{-1} \text{ cm}^{-1}$)³¹ was assumed for both AOT and PB solutions.

Results and discussion

Ground- and singlet excited state properties of flavins in RM

The absorption properties of flavins have received much attention either in homogeneous solvents or as cofactors in proteins.^{6–12} Two intense $\pi \rightarrow \pi^*$ absorption bands ($\epsilon_{\text{max}} \approx 10^4 \text{ M}^{-1} \text{ cm}^{-1}$) compose the UVA-Vis absorption spectrum of flavins, corresponding to the transitions from the ground state (S_0) to the lowest-lying excited states of the singlet manifold S_1 ($\lambda_{\text{max}} \sim 442\text{--}450 \text{ nm}$) and S_2 ($\lambda_{\text{max}} \sim 360\text{--}375 \text{ nm}$) of the isoalloxazine chromophore, respectively.^{5,9}

The general effect of the AOT RM milieu on the absorbance spectra of the flavins compared with homogeneous 10 mM sodium phosphate buffer (PB) solutions at pH 7 was the reduction of the molar absorption coefficient (ϵ_λ) together with hypsochromic shifts of both S_1 and S_2 bands, Fig. 1. These spectral changes were more intense for the S_2 band in the UVA. This behavior was similar to that reported for FMN in the interior of

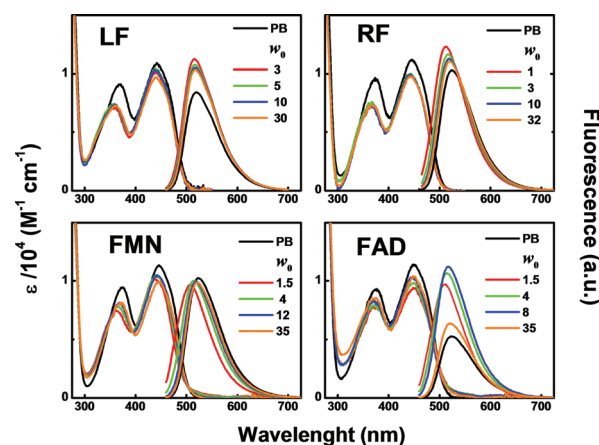


Fig. 1 UV-Vis absorption and emission spectra of approximately $7 \mu\text{M}$ lumiflavin (LF), riboflavin (RF), flavin mononucleotide (FMN), and flavin adenine dinucleotide (FAD) in 10 mM sodium phosphate buffer (pH 7) and in reversed micelles solutions of 0.1 M AOT in hexane at different water content, $w_0 = [\text{H}_2\text{O}]/[\text{AOT}]$. All emission spectra were corrected by the absorbance value at the excitation wavelength of 450 nm.

RM made with different surfactants.¹⁵ Furthermore, all flavins in AOT RM did not show the characteristic vibrational fine structure of the S_1 band as typically observed in apolar solvents,³² or as it was reported for the amphiphilic flavin derivative N(3)-undecylmiflavin anchored at the micellar interface of AOT RM.¹⁶

Conversely, UV-Vis spectral changes were almost independent of the AOT concentration (0.1–0.3 M) at fixed w_0 value. The above results suggest that the flavins are totally localized in the interior of RM, in contact with the water molecules of the water-pool. As a result, no partition effects of the flavins between the micellar interface and the external organic solvent would be expected by changing the concentration of RM.³³

Nevertheless, the increment of water content in the RM showed dissimilar effects depending on the flavin derivative. The absorbance spectra of LF and RF in RM were almost not modified by the increment of w_0 , in particular the S_2 band. In contrast, FMN showed progressive and modest red shifts (≈ 10 nm) of both bands with w_0 , together with modifications of the ε_λ values, in particular for the S_2 band. In the case of FAD, the increment of the water content did not change the positions of the bands, but gradually increased the ε_λ value of both bands. However, in all cases the absorbance spectrum of the flavins was not the same as that in PB solution, suggesting that the flavins are located in the aqueous interface of the interior waterpool, where the properties of the water molecules are not identical to bulk water.^{18,20,26}

For LF and RF in homogeneous solvents, it was reported that the $S_0 \rightarrow S_1$ transition is nearly independent of the surrounding solvent, although the $S_0 \rightarrow S_2$ band exhibits red shifts in polar and protic solvents.^{8,11,32} Recent CNDO/S calculations,³⁴ suggested that some mixing of an $n \rightarrow \pi^*$ transition involving the $N-1$ non-bonding electron pair with the $\pi \rightarrow \pi^*$ transition may occur. Thus, larger intensity of the 375 nm band on increasing the solvent polarity may be due to an increase in the

'allowedness' of this transition. The red shift observed on moving to protic solvents may reflect a destabilization of the $N-1$ non-bonding electrons by hydrogen bonding.^{8,9,34,35}

Only FMN and FAD in AOT solutions at low w_0 showed a small absorption band above 500 nm, Fig. 1. The shape of the difference absorbance spectrum (ΔA) of this band (see Fig. S1 of the ESI†) showed $\Delta A_{\max} \approx 510$ nm, the intensity of which decreased with the increment of w_0 . This result can arise from a small degree of charge-transfer interactions produced between the isoalloxazine ring of FMN and FAD and the sulfosuccinate ring group of AOT.

Therefore, the complex UV-Vis absorbance behavior of the flavins in AOT solution with w_0 can be understood mainly by changes of strength of the hydrogen bonding interactions of the isoalloxazine ring, probably at the N(1) and/or N(5) positions, with water molecules of the inner solvation shell of the micellar interface. The combination with specific charge-transfer interactions of the isoalloxazine ring with the polar head of the surfactant can be also considered, principally for FMN and FAD.

As shown also in Fig. 1, the fluorescence emission behavior in RM with w_0 was different for each flavin. For a more clear scrutiny, Fig. 2a–d summarizes the effect of w_0 on fluorescence quantum yields (Φ_F), Stokes shifts ($\nu_A - \nu_F$), full width of the half-maximum intensity (FWHM), and steady-state emission anisotropy ($\langle r \rangle$) of the flavins, compared with those values in PB solutions at pH 7. The emission parameter results obtained in PB solution were in good agreement with the literature data.^{5,8,9,11,12,36}

The fluorescence spectra of all flavins in AOT RM solution are characterized by broad structureless bands, but with spectral features depending on both the flavin derivative and w_0 . The Φ_F values for all flavins in RM were larger than in PB solution, Fig. 2a, as expected for fluorophores in more viscous or rigid media. For LF, RF and FMN, Φ_F slightly decreases with the increment of the dispersed water. In contrast, the variation of Φ_F

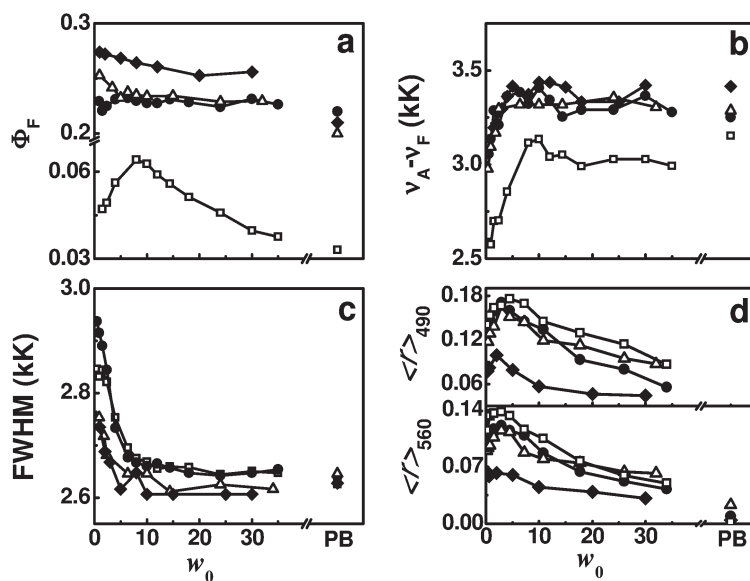


Fig. 2 Variation of the fluorescence parameters of 7 μ M flavins in AOT 0.1 M-n-hexane solutions as function of the water content (w_0) and in 10 mM sodium phosphate buffer (PB) solution at pH 7: (a) fluorescence quantum yields (Φ_F); (b) Stokes shifts ($\nu_A - \nu_F$); (c) full width of the half-maximum intensity (FWHM) of the emission band; (d) and average emission anisotropy at 490 ± 5 nm ($\langle r \rangle_{490}$) and 560 ± 5 nm ($\langle r \rangle_{560}$). Symbols: (◆) lumiflavin, LF; (△) riboflavin, RF; (●) flavin mononucleotide, FMN; and (□) flavin adenine dinucleotide, FAD.

with w_0 for FAD showed a maximum value at $w_0 \approx 8$, to subsequently decrease to a value close to that observed in PB solution.

All flavins showed similar increments of the Stokes shifts ($\nu_A - \nu_F$) with w_0 , reaching a plateau at $w_0 \approx 5-10$ with values closer to those observed in PB solution for each flavin, Fig. 2b. This result indicates the progressive stabilization of the emitting excited state of the flavins with the increment of dispersed water into the RM. The effect of protic homogeneous solvents on the Stokes shifts of the flavins was also analyzed as a function of the orientation polarizability (Δf) (Fig. S2 of ESI†), according to the well-known Mataga–Lippert (M–L) equation.³⁷ Only LF showed good correlation of the M–L equation for solvents with $\Delta f \leq 0.3$. However, a strong positive deviation for highly polar solvents with $\Delta f \geq 0.3$ (e.g. methanol and water) was observed, which is assigned to specific hydrogen-bonding interactions.³⁸ Conversely, the other flavins showed large Stokes shift values independently of the Δf of the protic solvents, probably by the effect of the pendant ribityl group in the isoalloxazine ring. Therefore, the large Stokes shift values of all flavins observed in RM can indicate the prevalence of strong hydrogen-bonding interactions of the isoalloxazine ring with water molecules of the micellar interior. The occurrence of specific interactions by acid–base equilibrium effects of the flavins in the interior of the RM can be neglected due to the pH control of the waterpool with the PB solution at pH 7, and the very low pK_a values (<2) of both ground and excited singlet states of the flavins.^{5,36}

Therefore, specific interactions in the interior of the RM seem to play a role in the spectroscopic properties of the flavins. In the present case, those specific interactions are expected to occur at both the ground and singlet excited state of the flavins, since both absorbance and fluorescence spectra were modified in AOT solutions.

The FWHM variation with w_0 indicates that all flavins showed a progressive spectral narrowing up to $w_0 < 10$, Fig. 2c. However, in these conditions, the emission spectra of both FMN and FAD were a little broader than for LF and RF. At $w_0 > 10$, the emission spectral width for all flavins was similar to those observed in PB. This result points out the possibility of larger heterogeneity in the emitting properties of the flavins in the micellar core at $w_0 < 10$, since the FWHM of the flavins in homogeneous media is nearly independent of the solvent properties.

The changes of the steady-state fluorescence anisotropy $\langle r \rangle$ of the flavins in RM was considerably larger than in PB solution, as a result of the enhanced viscosity of the entrapped water in the interior of the RM.^{15,22–24,39} However, $\langle r \rangle$ was dependent on the monitoring emission wavelength, since the anisotropy values calculated at the blue-edge of the emission spectrum (e.g. 490 ± 5 nm, $\langle r \rangle_{490}$) were significantly larger ($>30\%$) than those values calculated at the red-edge of the emission spectrum (e.g. 560 ± 5 nm, $\langle r \rangle_{560}$), Fig. 2d. This result could be indicative of solvent relaxation effects, by which the anisotropy decreases with increasing wavelength because the average lifetime is longer for longer wavelengths.⁴⁰ If this is the case, this effect is generally observed when the solvent relaxation time is comparable to the fluorescence lifetime.²⁸

All flavins showed similar variation of $\langle r \rangle$ with w_0 , reaching a maximum value at $w_0 \approx 5$. However, for LF the anisotropy

was significantly lower than for the rest of the flavins. To compare, the anisotropy of LF and FMN in neat glycerol ($\eta \approx 1400$ cp at 20 °C) was estimated approximately as 0.28 and 0.40, respectively, and with $<5\%$ of diminution between the blue- and red edges of the fluorescence spectra (Fig. S3 of ESI†). Therefore, the intrinsic anisotropy of LF is about 30% less than that of FMN in homogeneous solvents explaining its smaller value in RM.

The internal viscosity of the AOT RM has been estimated to decrease from approximately 380 to 4 cp changing w_0 between 2 and 50; respectively, with the micellar interface being more viscous than the waterpool.^{22,24} Similarly to the behavior observed for other anisotropy probes attached to the AOT micellar interface,^{22,39} the initial increment of $\langle r \rangle$ for RF, FMN and FAD with w_0 can be associated with the overall rotation of the RM, since the internal rotation of the flavin is hindered by the high internal viscosity. As the diameter of the RM increases with w_0 , the rotation of the whole system is slowed and the fluorescence depolarization of the probe is delayed. However, the increment of w_0 parallels with the diminution of the internal viscosity of the RM allowing the internal rotation of the flavins and the increase of the depolarization.¹⁵ Thus, the combination of both effects explains the existence of an anisotropy maximum at $w_0 \approx 5$, Fig. 2d. This assumption was confirmed by time-resolved anisotropy experiments presented in the following section.

As already observed for several molecules and molecular complexes,^{33,41,42} all the above results indicate the effect of specific interactions of the flavins in the internal micellar interface, which depends on the increment of the size and fluidity of the RM governed by the hydration degree of the micellar interface. This assumption is supported by the time-resolved fluorescence experiments presented in the following section.

Fluorescence dynamic behavior of the flavins in RM

In PB solution, the fluorescence decay of LF, RF, FMN was single exponential with lifetimes according to literature data.^{5,8,11,12,15} In contrast, FAD displayed double-exponential decay, due to the decay of the “stacked” and “open” conformers formed by intramolecular interaction of the isoalloxazine ring with the adenine moiety.^{12,36,43,44}

The fluorescence decay of the flavins in AOT solutions showed double-exponential behavior, with decay times (τ_i) and fluorescence intensity amplitudes at $t = 0$ (α_i) depending on the amount of water dispersed in the RM.^{15,39} As an example, Fig. 3a illustrates a typical double-exponential fluorescence decay at 520 nm of FMN in RM at $w_0 = 20$. Fig. 3b–e show the variation with w_0 of both the fractional contribution of each decay time (f_i) and the average lifetime $\langle \tau \rangle$ calculated with eqn (3). For LF, RF and FMN, the fluorescence decay contained significant double-exponential contributions at $w_0 < 5-8$. Above this value, the fluorescence intensity of these flavins decayed practically as a single exponential. In contrast, FAD showed double exponential behavior independently of w_0 , according to its intramolecular quenching effect by the adenine moiety.^{36,39} Considering the changes in the relative contributions to the double-exponential behavior of the fluorescence decays of the flavins in RM, $\langle \tau \rangle$ is a useful magnitude to provide a simpler

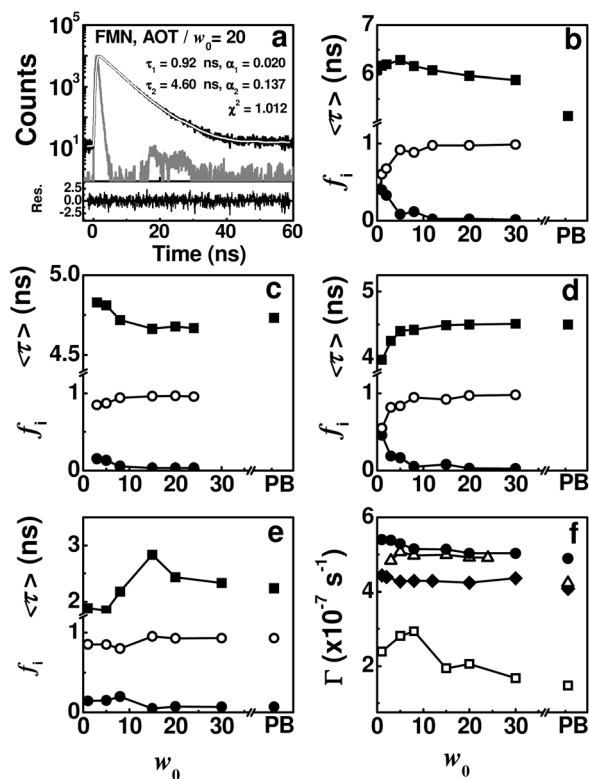


Fig. 3 (a) Decay of fluorescence of 7 μM FMN at 520 nm in air-saturated 0.1 M AOT-n-hexane/ $w_0 = 20$ solutions obtained with ultrafast Nanoled® excitation at 340 nm. (b–e) Variation of the fractional contribution of each decay time, f_i (●, ○), and average lifetime τ_{av} (■) observed at 520 nm for LF (b); RF (c); FMN (d); FAD (e). (f) Radiative rate constant $\langle\Gamma\rangle = \Phi_F/\langle\tau\rangle$ of (◆) LF; (△) RF; (●) FMN; and (□) (FAD).

way of illustrating the overall decay variations. The change of $\langle\tau\rangle$ with w_0 was different for each flavin. A slight decrease of $\langle\tau\rangle$ up to $w_0 \approx 5$ was observed for LF and RF. However, $\langle\tau\rangle$ of LF at larger w_0 was longer than in PB solutions and similar to those values observed in less polar organic solvents,⁸ confirming a probe localization in a less polar region of the waterpool. Furthermore, the $\langle\tau\rangle$ values for LF were 25–30% longer than for the other flavins in RM. This variation contributes to lower anisotropy values according to the Perrin formula for anisotropy, *i.e.* $r_0/\langle r \rangle - 1 = \langle\tau\rangle/\theta$, assuming similar rotational correlation times (θ).^{15,16,22–24} This assumption was checked by time-resolved anisotropy experiments of LF and FAD in AOT RM with excitation at 340 nm. Fig. 4 shows the emission anisotropy decay of LF at $w_0 = 2$. For both flavins at the different w_0 values, the anisotropy decay was exponential and it was fitted with eqn (4) to obtain r_0 and θ , Table 1. These parameters were similar to those reported for FMN in AOT RM in iso-octane,¹⁵ in which also exponential decay of fluorescence anisotropy was observed. This kinetic behavior of the anisotropy decays confirms that the flavins are not partitioned between different nanophases of the RM, since in that case multiexponential decay behavior of anisotropy can be anticipated. The inset of Fig. 4 shows that both LF and FAD presented similar variation of θ with w_0 , with a maximum value at $w_0 = 2–3$, similarly to that observed for $\langle r \rangle$,

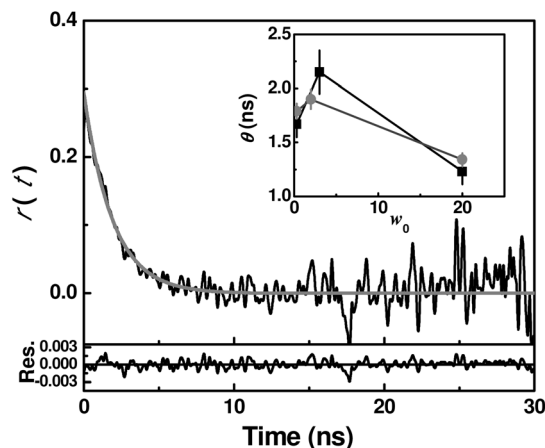


Fig. 4 Decay of fluorescence anisotropy of 7 μM LF in air-saturated 0.1 M AOT-n-hexane/ $w_0 = 2$ solutions monitored at 520 nm and obtained with ultrafast Nanoled® excitation at 340 nm. The gray line represents the fitting function with eqn (4). Inset: variation with w_0 of the rotational correlation time θ (ns) of LF (gray circles) and FAD (black squares).

Table 1 Anisotropy characteristics of lumiflavin (LF) and flavin adenine dinucleotide (FAD) in 0.1 M AOT-n-hexane–water reversed micelles at different $w_0 = [\text{H}_2\text{O}]/[\text{AOT}]$ values at 25 °C

Flavin	w_0 (R_h , nm) ^a	$\langle r \rangle^b$	r_0	θ (ns)	θ_m (ns) ^c	θ_i (ns) ^d
LF	0.3 (1.8)	0.062	0.37 ± 0.08	1.7 ± 0.1	1.7	63
	2.0 (2.0)	0.079	0.29 ± 0.04	1.9 ± 0.1	2.4	8.3
	20 (5.0)	0.042	0.24 ± 0.01	1.4 ± 0.1	37.4	1.4
FAD	0.3 (1.8)	0.110	0.28 ± 0.03	1.7 ± 0.1	1.7	38
	3.0 (2.3)	0.149	0.27 ± 0.09	2.2 ± 0.2	3.8	5.0
	20 (5.0)	0.086	0.22 ± 0.03	1.2 ± 0.1	37.4	1.3
FMN ^e	3.8 (2.5)	0.175	0.31	3.8	8.8	6.7
	28.7 (5.5)	0.075	0.23	1.6	93.3	1.6

^a Hydrodynamic radii of AOT RMs from ref. 19. ^b Steady-state anisotropy at 520 nm. ^c Rotational correlation time of the spherical reversed micelle calculated as $\theta_m = 4\pi R_h^3 \eta / (3kT)$, with $\eta_{\text{hexane}} = 0.294$ cp at 25 °C. ^d From $\theta_i^{-1} = \theta^{-1} - \theta_m^{-1}$ (ref. 15). ^e Data from ref. 15 for 0.1 M AOT in n-octane

Fig. 2d. We followed the elegant analysis performed by Visser *et al.* for FMN in AOT-n-octane RM,¹⁵ to separate from the experimental θ value the uncoupled rotational correlation times corresponding to the rotation of the whole micelle (θ_m) and that for the internal flavin (θ_i), Table 1. As expected, the increment of the micellar size increased θ_m with the simultaneous diminution of θ_i , explaining the bell-shaped variation of both $\langle r \rangle$ and θ , Fig. 2d and 4. Furthermore, the calculated θ_i values for LF and FAD were in the trend for the reported values of FMN in AOT-n-octane at similar w_0 , confirming that the interior properties of the reversed micelles are independent of both the surfactant concentration and the external organic solvent. The difference in $\theta_m = 4\pi R_h^3 \eta / (3kT)$,¹⁵ can be assigned to the larger viscosity of n-octane ($\eta \approx 0.54$ cp) compared with n-hexane ($\eta \approx 0.29$ cp) at room temperature.

Conversely, the $\langle\tau\rangle$ values of FMN increased up to $w_0 < 10$, while for FAD a maximum value at $w_0 \approx 4$ was observed. In both cases, the average lifetime at larger w_0 approached to the value in PB solution. The average radiative decay rate, *i.e.* $\langle\Gamma\rangle = \Phi_f/\langle\tau\rangle$, for LF, RF, and FMN was independent of w_0 and the same than in PB solution for each flavin, Fig. 3f. Thus, the rate of the radiative pathway of these flavins does not depend on the changes of the internal nanoenvironmental properties of the RM. However, FAD showed a maximum $\langle\Gamma\rangle$ at $w_0 \approx 6-8$, as a result of the variation of its fluorescence quantum yield and average lifetime with w_0 , Fig. 2a and 3e, respectively. A possible explanation for this anomalous behavior of FAD inside RM can arise from a combination of inter- and intramolecular quenching effects. At very low w_0 values (*e.g.* ≤ 5) the interaction of FAD with the AOT polar heads and sodium counterions enhances intermolecular quenching effects of the isoalloxazine ring. As w_0 increases, the solvation of the micellar interface reduces this effect and the intramolecular quenching process of FAD dominates the dynamic behavior of the isoalloxazine ring, which progressively shifts from the “unstacked” to “stacked” form as the microviscosity decreases with w_0 .

Besides the effect of w_0 for the different flavins, the fluorescence decays in AOT solutions were also dependent on the monitoring emission wavelength, with faster decays at the blue edge of the emission spectrum. The same effect was observed

for 3-methylflavin in propylene glycol as a function of temperature,⁴⁰ which was explained by dipolar solvent relaxation effects.

The complex wavelength-dependent decay behavior of the flavins in AOT RM is sketched for FMN in Fig. 5 by the representation of the decay associated spectra (DAS) and the normalized time-resolved emission spectra (TRES) at $w_0 = 1$ and 20, respectively. In RM solutions with very low w_0 values (*e.g.* $w_0 < 3$), two well defined DAS bands were observed with emission maxima around 487 nm and 512 nm, respectively, confirming the emission from at least two different excited-states populations of the flavins. At $w_0 = 20$, the main DAS component corresponded to the long-lived red-emitting species ($\lambda \approx 520$ nm). These results are compatible with the polarity and fluidity increments of the solvation sphere of FMN as w_0 increases.^{18–26,42} Table 2 collects the DAS parameters for the blue- and red-shifted bands of the flavins in AOT solutions as a function of w_0 . In all cases, the blue-shifted emission ($\lambda_b = 492-505$ nm) showed smaller decay time (τ_b) and relative emission area (F_b) than those (*e.g.* τ_r and F_r) for the red-shifted emission band ($\lambda_r = 512-525$ nm). At $w_0 = 1$, the relative amount of the blue emitting species was in the order FAD > FMN > RF > LF. However, the amount of the blue-emitting species was strongly depleted together with shortening of the associated decay time τ_b with the increment of w_0 . Instead, the decay time

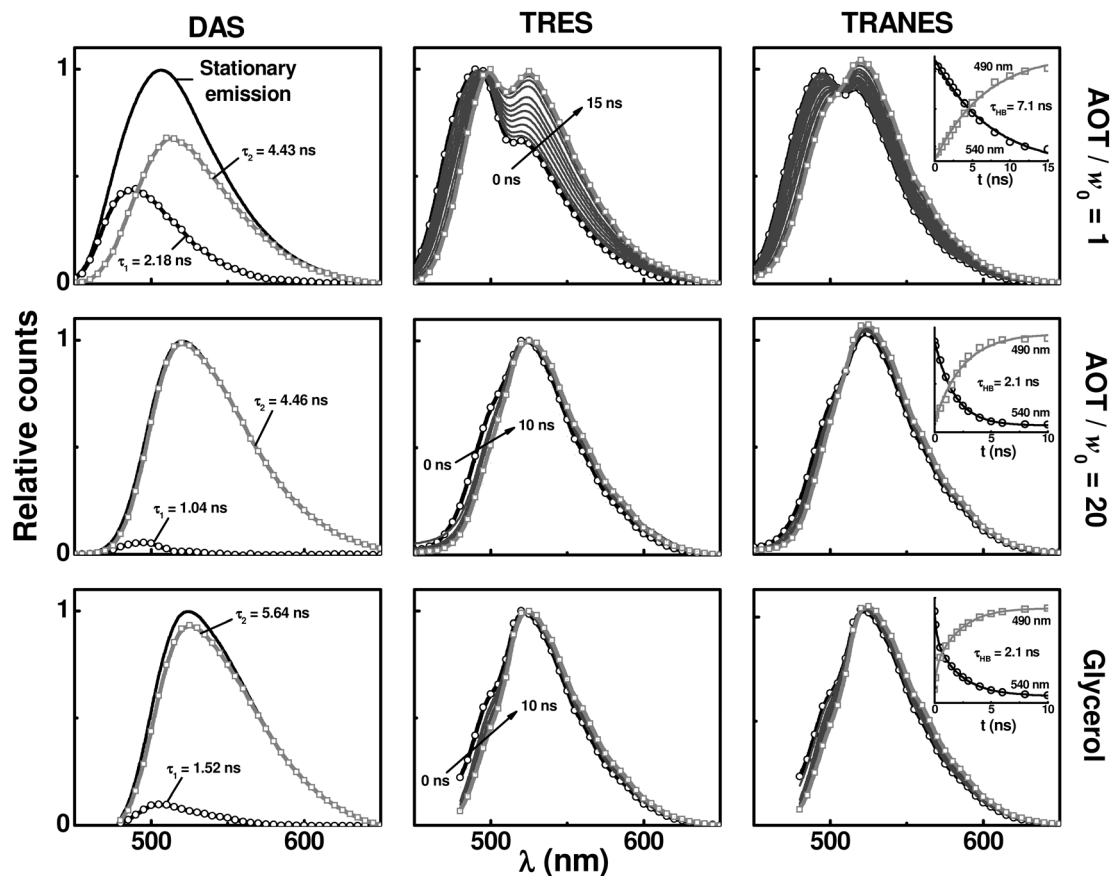


Fig. 5 Time-resolved emission behavior of 7 μM flavin mononucleotide (FMN) in 0.1 M AOT-n-hexane at $w_0 = 1$ (top) and = 20 (center), and in glycerol (bottom) represented as the decay associated spectra (DAS, left column); the normalized time-resolved emission spectra (TRES, center column), and the time-resolved area normalized emission spectra (TRANES, right column). Insets in TRANES plots: kinetic profile associated with the decay and formation of the hydrogen bonding unrelaxed (490 nm) and relaxed (540 nm) singlet excited state of FMN (see text and Scheme 2).

Table 2 Relative emission area (F_r), emission maxima (λ_i , nm), and decay times (τ_i , ns), of the decay associated spectra (DAS); and isoemissive points (λ_{ic}) and relaxation time for hydrogen-bonding formation at the excited state (τ_{HB} , ns) obtained by time-resolved area normalized spectroscopy (TRANES) of air-saturated solutions of flavins in 0.1 M AOT–n-hexane–water reversed micelles and glycerol at 25 °C^a

Flavin	w_0	F_b	λ_b	τ_b	F_r	λ_r	τ_r	λ_{ic}	τ_{HB}^b
LF	1	0.21	495	3.07	0.79	514	6.93	507	8.5 ± 0.5
	8	0.07	495	1.19	0.93	517	6.28	508	1.8 ± 0.1
	20	0.02	492	1.05	0.98	517	6.02	508	1.6 ± 0.2
RF	1	0.25	493	2.39	0.75	515	5.32	506	4.6 ± 1.1
	8	0.08	492	1.13	0.92	518	4.88	509	1.9 ± 0.1
	20	0.06	493	1.07	0.94	519	4.80	509	1.7 ± 0.1
FMN	1	0.34	487	2.18	0.66	512	4.43	507	7.1 ± 0.1
	8	0.11	493	1.98	0.91	518	4.45	509	2.0 ± 0.1
	20	0.02	495	1.04	0.98	520	4.46	509	1.0 ± 0.3
	Glycerol	0.06	505	1.52	0.94	525	5.64	514	2.1 ± 0.1
FAD	1	0.38	494	0.28	0.62	512	2.16	504	6.2 ± 0.1
	8	0.05	502	0.24	0.95	518	2.83	509	2.4 ± 0.1
	20	0.04	500	0.23	0.96	520	2.61	511	2.2 ± 0.2

^a The subscripts **b** and **r** indicate blue-shifted (unrelaxed) and red-shifted (relaxed) emitting species. Standard deviation, ±5%. ^b Average values from the decay and growth of TRANES at 475 nm and 540 nm, respectively.

of the red emitting species (τ_r) was almost constant with w_0 , despite of the growth of its relative population (F_r), Table 2.

The prompt ($t = 0$ ns) normalized TRES slice in AOT RM at $w_0 = 1$ showed the combined dual emission with maxima around 490 nm and 520 nm, with larger intensity for the blue shifted band. The evolution of the normalized TRES of FMN after 15 ns shows that the decay of emission at 490 nm occurred with a 10 nm red shift of its emission maximum, simultaneously with the relative increment of the band at 520 nm, Fig. 5. At larger w_0 values, the TRES of FMN was dominated by the emission of the red emitting species. Similar results were observed for the other flavins in AOT RM solutions. However, all flavins in PB solutions showed TRES identical to its stationary spectra (see Fig. S4 of ESI† for FMN), as it can be expected for completely solvent relaxed excited states.

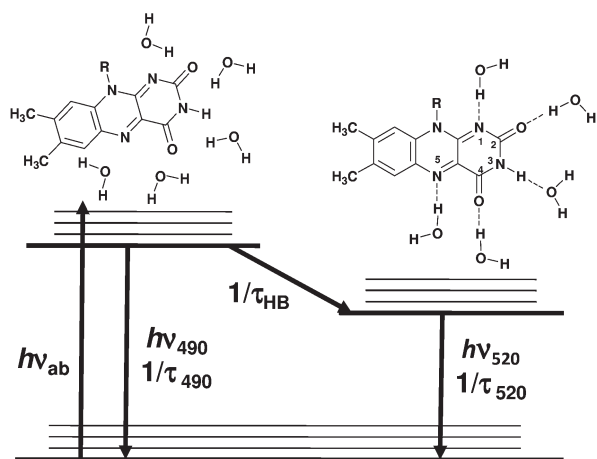
The time-resolved behavior of FMN as model flavin in highly viscous glycerol was also analyzed, and it was found to be similar to that observed in AOT solutions at $w_0 = 20$, Fig. 4. However, the internal viscosity of the AOT RM was estimated around 3–5 cp at $w_0 = 20$,^{22,24} a very small value compared with glycerol viscosity at room temperature ($\eta \approx 1400$ cp). This result confirms that the singlet excited-state properties of the flavins in the RM are governed by specific solvent interactions rather than by local viscosity effects.

It is worthy of note that the prompt TRES of the flavins in AOT RM resemble to the steady-state fluorescence spectrum of flavins in aprotic solvents,^{6,32} as is shown for LF in dry toluene (Fig. S5 of ESI†), and also for FMN in protein cavities, such as in the LOV domain of the wild type and mutants of the blue-light receptor YtvA of *Bacillus subtilis*.⁴⁵ In this protein, the FMN is highly stabilized and immobilized by a hydrogen bond network involving several amino acids of the active site, where water solvent molecules are excluded.⁴⁵ Therefore, the nature of the hydrogen-bonding partner of the isoalloxazine ring also plays a role in the emission properties of the flavins. In fact, Yagi *et al.*⁶ reported that the effect on the steady-state fluorescence spectrum of riboflavin tetrabutryrate in dry CCl₄ of increasing the hydrogen bonding strength by the addition of trichloroacetic or trifluoroacetic acids was the loss of the vibrational maximum at

the blue (approximately at 490–500 nm) together with the diminution of the fluorescence quantum yield.

Therefore, taking all results together, the spectroscopic behavior of the flavins in AOT RM solutions can be interpreted as a function of a dynamic solvent relaxation process,^{40,46} in which hydrogen bonding interactions are involving in the relaxation of excited state of the flavins, Scheme 2. In the present case, the blue-edge emitting species ($\lambda_b < 500$ nm) is an unrelaxed (Franck–Condon) non-hydrogen bonding state, which decays in parallel to the ground state and to the hydrogen bonding (solvent relaxed) excited state, which emits at the red edge of the spectrum ($\lambda_r > 500$ nm). At higher water content in the AOT solution (*e.g.* $w_0 = 20$), the hydrogen-bonded solvated excited state of the flavin is practically the main emitting species ($\lambda_{max} = 520$ nm).

As mentioned before, the properties of water in AOT RM at low w_0 values are rather different from those of bulk water.^{19–26} Three types of water populations (pools) have been shown to coexist in the interior of reverse micelles. These are the water molecules involved in the solvation of the polar heads of the surfactant, the trapped water shell between the micellar interface and the core of the waterpool, and the free water molecules in the center of the waterpool. The relative proportions of these types of water are determined by w_0 .^{18–26} At low w_0 (<6) most water molecules are immobilized in the solvation of the anionic polar heads of AOT and sodium counterions, and the proportion of hydrogen-bonded aqueous matrix is minimal.^{20,25} Under this condition, the water molecules of the waterpool have reduced mobility to form hydrogen-bonding interactions with the lone electron pairs of the heteroatoms of the isoalloxazine ring of the flavins and the unrelaxed non-hydrogen bonding state is produced upon excitation. Upon increasing the w_0 a greater amount of hydrogen bonding network with larger mobility and strength is found in the aqueous matrix of the waterpool, as was determined by laser-induced optoacoustics using the hydrogen-bonding sensitive metal complex Ru(bpy)(CN)₄^{2–}.²⁵ Therefore, at large w_0 values, almost complete prompt hydrogen bonding stabilization of the excited state of the flavins is expected, as typically occurs in fluid polar solvent solutions.



Scheme 2 Jablonski diagram for the hydrogen-bonding stabilization of the unrelaxed (blue-emitting species) to the relaxed (red-emitting species) of the flavins in the interior of AOT reversed micelles. Both rotational reorganization of the isoalloxazine ring and hydrogen-bonding relaxation occur simultaneously. Hydrogen-donor and acceptor water molecules involved are those from the solvation inner shell of the AOT RM, the amount and bonding strength of which increases with the w_0 ($= [H_2O]/[AOT]$) value.

In order to estimate the dynamic parameters of the hydrogen-bonding relaxation around the singlet excited state of the flavins in RM solutions, the time-resolved area normalized emission spectra (TRANES) were calculated from the experimental TRES.²⁹ The advantage of this procedure is to overcome the prior knowledge of the number of fluorescent species in the ground state required in the standard kinetic interpretation of TRES.⁴⁷ This requirement is difficult to fulfil in complex environments such as microheterogeneous media. Instead, in TRANES no assumptions of any ground or excited-state kinetics are necessary, with the extra advantage that the presence of an isoemissive point in the spectra supports any model that involves two emitting species in the sample.²⁹ Fig. 5 shows the TRANES spectra for FMN in AOT RM solutions and in glycerol. A clear isoemissive point (λ_{ie}) around 508 nm and 514 nm was observed for AOT RM and glycerol, respectively, supporting the presence of two emitting states of the flavins in these media. The same behavior was observed for the others flavins, Table 2. The kinetic analysis of the TRANES evolution allowed the calculation of the decay time for the hydrogen bonding formation (relaxation) in the excited state of the flavins, τ_{HB} , Fig. 5 and Table 2. The calculated τ_{HB} was coincident with the internal rotational correlation time (θ_i) of the flavins at similar w_0 , *i.e.* approximately between 7 and 1.5 ns by changing w_0 from 1 to 20, respectively. This result suggests that the unrelaxed excited state of the flavin is reoriented during the stabilization by the hydrogen bonding interactions.

Triplet state properties in RM

The prompt transient spectrum of the flavins (50 μ M) after the laser pulse at 355 nm in deaerated 0.3 M AOT RM and in 10 mM PB solutions by Ar-bubbling, showed the typical transient triplet-to-singlet difference absorption spectra of the flavins,

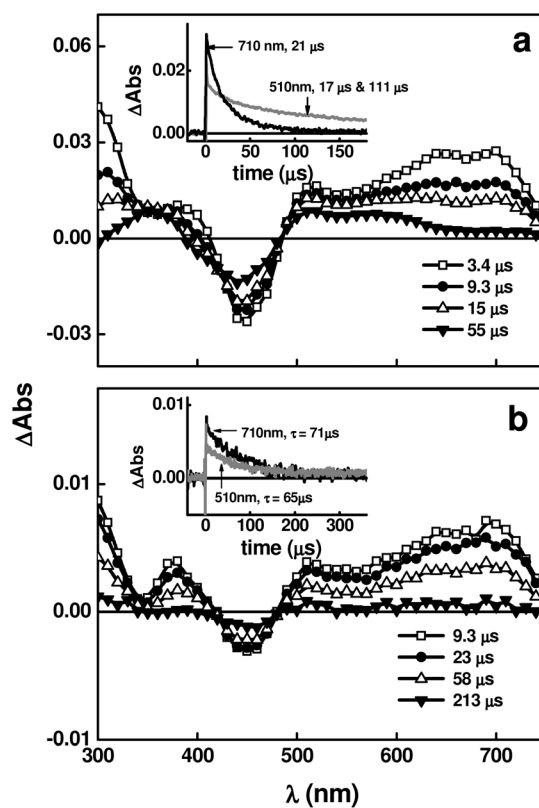


Fig. 6 Transient absorption spectra of 50 μ M riboflavin (RF) in Ar-saturated 10 mM sodium phosphate buffer (PB) solution at pH 7 (a); and in 0.3 M AOT-n-hexane at $w_0 = 3$ (b) obtained after laser excitation at 355 nm. Insets show the kinetic profile observed at 510 and 710 nm, respectively.

which is characterized by the broad absorption band of the triplet state with vibrational transitions at 715 and 660 nm.^{5,30,31}

In Ar-bubbled homogeneous PB solutions, the triplet state of the flavins decayed with lifetime values according to the literature data.^{5,30,31,48,49} Fig. 6a shows the transient spectrum of RF, in which the $^3\text{RF}^*$ decays in 21 μ s ($k_d = \tau_T^{-1} = 4.8 \times 10^4 \text{ s}^{-1}$) forming the semiquinone radical (500–650 nm band) by self-quenching of the triplet state by ground state flavin molecule with rate constant of $\approx 2 \times 10^8 \text{ M}^{-1} \text{ s}^{-1}$.⁴⁹ Subsequently, this species yielded bleaching products with a lifetime of 111 μ s, Fig. 6a. On the contrary, in AOT RM solutions the $^3\text{RF}^*$ showed longer lifetimes ($\tau_T = 71$ and 54 μ s at $w_0 = 3$ and 20, respectively) than in homogeneous PB solutions, and decayed without forming the semiquinone species, as shown in Fig. 6b for $w_0 = 3$. This result suggests that in RM solutions the rate of the self-quenching process is avoided by the micellar organization. Considering the aggregation numbers of AOT in n-hexane (≈ 50 and 290 at $w_0 = 3$ and 20, respectively),²⁰ the ratio between the concentration of flavin and reverse micelles, *e.g.* $[\text{Flavin}]/[\text{RM}]$, changed between 0.008 and 0.048 for $w_0 = 3$ and 20, respectively. Therefore, the interaction between two flavin molecules in the same micellar assembly is highly avoided under these concentration conditions. However, by analyzing the bleaching band of the flavin at 450 nm, it can be noted that the ground state concentration is not completely recovered at the end of the triplet state decay, suggesting the occurrence of unimolecular photo-bleaching pathways.⁵⁰

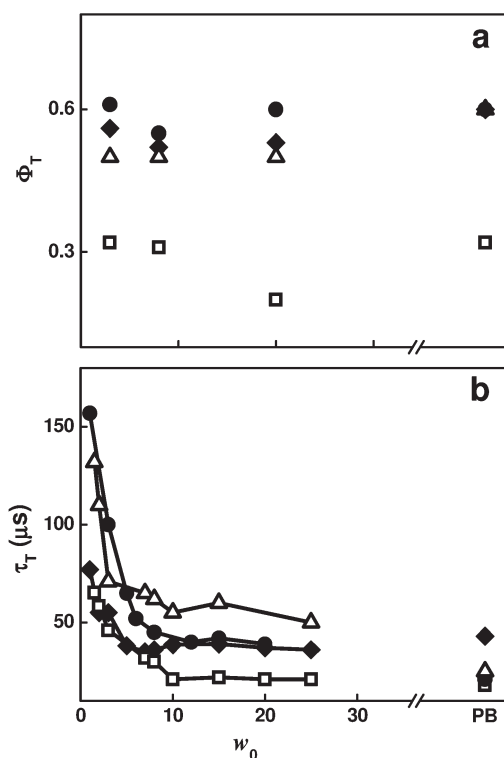


Fig. 7 Triplet quantum yield (Φ_T) and lifetimes (τ_T) of flavins in Ar-saturated 0.3 M AOT-n-hexane as function of the water content (w_0) and in 10 mM sodium phosphate buffer (PB) solution at pH 7 for: (◆) lumiflavin, LF; (△) riboflavin, RF; (●) flavin mononucleotide, FMN; and (□) flavin adenine dinucleotide, FAD.

Fig. 7 shows the effect of w_0 on the triplet state properties of the flavins. As well as the quantum yield of triplet formation (Φ_T) value of the flavins being nearly independent of w_0 and similar to that observed in PB solutions, a large shortening of the triplet lifetime (τ_T) at $w_0 < 10$ was observed for all flavins. The same relative variation of the τ_T values with w_0 was observed in air-saturated AOT RM solutions (data not shown), despite of the fact that the triplet lifetime of the flavins was efficiently quenched by molecular oxygen ($k_Q \approx 1 \times 10^9 \text{ M}^{-1} \text{ s}^{-1}$).⁵¹ Therefore, the effect of w_0 on the triplet lifetimes of the flavins can be ascribed to specific changes of the interior of the RM rather than by effect of quenching by molecular oxygen impurity.

It is interesting to compare the triplet state behavior of FMN in RM with that observed in the LOV domains of a series of YtvA protein mutants.⁴⁵ It was reported that the specific mutation of the wild-type protein of the highly conserved Asp 94 by Ala changes noticeably the triplet lifetime of FMN from 2 to 129 μs , without significant modifications of Φ_T (≈ 0.6). In this case, it was claimed that the changes in the amino-acid hydrogen bonding network of YtvA affected specifically the microenvironment around the N(5) of the isoalloxazine ring of FMN.⁴⁵ Therefore, both sets of independent results point out that the triplet lifetime of flavins very much depends on the environmental rigidity and/or on the nature of the hydrogen donor partner interacting with the isoalloxazine ring. In fact, the τ_T of the flavins in AOT RM decreases proportionally with the relative amount of

hydrogen-bonding relaxed species (F_T), Table 2, supporting the effect of the composition and strength of the hydrogen-bonding network inside of the RM on the triplet state properties of the flavins.

Conclusions

We have presented steady-state and dynamic spectroscopic experimental evidence that hydrogen-bonding interactions produced by confined water molecules in AOT RM modulate both singlet and triplet excited properties of flavins. The spectroscopic control is governed by the hydration degree of the micellar interior, given by the water-to-surfactant molar ratio w_0 ($= [\text{H}_2\text{O}]/[\text{AOT}]$). A dynamic solvent relaxation model was proposed, in which a blue-edge emitting ($\lambda_b < 500 \text{ nm}$) unrelaxed singlet state decays in parallel to the ground state and to a red-emitting singlet state ($\lambda_r > 500 \text{ nm}$) by formation of hydrogen-bonding interactions with the lone electron pairs of the heteroatoms of the isoalloxazine ring of the flavins.

The analysis of the fluorescence anisotropy decays and TRANES of the flavins in AOT RM confirmed that both the internal rotational time of the flavins θ_i and the hydrogen-bonding relaxation time τ_{HB} were coincident and decreased approximately from 7 ns and 1.5 ns at $w_0 = 1$ and 20, respectively. Therefore, it can be concluded that the reorientation of the unrelaxed singlet excited state of the flavins is controlled by the ability of the water molecules to form hydrogen bonds.

The triplet state lifetime of the flavins was also enlarged in AOT RM solutions at low w_0 , without modifications of the triplet quantum yields. The changes of the dynamics of the triplet state decay of the flavins can be related with the global composition and strength of the hydrogen-bonding network inside of the RM.

Finally, some dynamic aspects of the photophysical behavior of both singlet and triplet excited states of the flavins in AOT RM resembled those observed in flavoproteins.⁴⁶ This feature makes of RM an attractive model system of biological organized structures, such as protein cavities and biomembranes, since RM mimic some important and essential features of these biological systems although lacking much of their associated complexity by simply changing of the amount of dispersed water, *i.e.* w_0 .

Acknowledgements

The authors thank the Argentinean Funding Agencies CICyT-UNSE, CONICET, and ANPCyT (PICT-06-01090) for their financial support. CDB thanks also the Alexander von Humboldt Foundation for a Georg Foster Fellowship.

References

- 1 S. Bornemann, Flavoenzymes that catalyse reactions with no net redox change, *Nat. Prod. Rep.*, 2002, **19**, 761–772.
- 2 A. Losi, Flavin-based blue-light photosensors: a photobiophysics update, *Photochem. Photobiol.*, 2007, **83**, 1283–1300.
- 3 M. A. Montenegro, I. L. Nunes, A. Z. Mercadante and C. D. Borsarelli, Photoprotection of vitamins in skimmed milk by aqueous soluble lycopene – gum arabic microcapsule, *J. Agric. Food Chem.*, 2007, **55**, 323–329.

- 4 I. Ahmad, Q. Fasihullah, A. Noor, I. A. Ansari and Q. N. M. Ali, Photolysis of riboflavin in aqueous solution: a kinetic study, *Int. J. Pharm.*, 2004, **280**, 199–208.
- 5 P. F. Heelis, The photophysical and photochemical properties of flavins (isoalloxazines), *Chem. Soc. Rev.*, 1982, **11**, 15–39.
- 6 K. Yagi, N. Ohishi, K. Nishimoto, J. D. Choi and P. S. Song, Effect of hydrogen-bonding on electronic-spectra and reactivity of flavins, *Biochemistry*, 1980, **19**, 1553–1557.
- 7 F. Müller, S. G. Mayhew and V. Massey, On the effect of temperature on the absorption spectra of free and protein-bound flavines, *Biochemistry*, 1973, **12**, 4654–4662.
- 8 E. Sikorska, I. V. Khmelinskii, W. Prukala, S. L. Williams, M. Patel, D. R. Worrall, J. L. Bourdelande, J. Koput and M. Sikorski, Spectroscopy and photophysics of lumiflavins and lumichromes, *J. Phys. Chem. A*, 2004, **108**, 1501–1508.
- 9 M. Kowalczyk, E. Sikorska, I. V. Khmelinskii, J. Komasa, M. Insinska-Rak and M. Sikorski, Spectroscopy and photophysics of flavin-related compounds: isoalloxazines, *J. Mol. Struct. (THEOCHEM)*, 2005, **756**, 47–54.
- 10 K. Zenichowski, M. Gothe and P. Saalfrank, Exciting flavins: absorption spectra and spin-orbit coupling in light-oxygen-voltage (LOV) domains, *J. Photochem. Photobiol., A*, 2007, **190**, 290–300.
- 11 P. Zirak, A. Penzkofer, T. Mathes and P. Hegemann, Photo-dynamics of roseoflavin and riboflavin in aqueous and organic solvents, *Chem. Phys.*, 2009, **358**, 111–122.
- 12 Y. T. Kao, C. Saxena, T. F. He, L. J. Guo, L. J. Wang, A. Sancar and D. P. Zhong, Ultrafast dynamics of flavins in five redox states, *J. Am. Chem. Soc.*, 2008, **130**, 13132–13139.
- 13 W. Schmidt, Environment and the rotational motion of amphiphilic flavins in artificial membrane-vesicles as studied by fluorescence, *J. Membr. Biol.*, 1979, **47**, 1–25.
- 14 W. Schmidt, Further photophysical and photochemical characterization of flavins associated with single-shelled vesicles, *J. Membr. Biol.*, 1983, **76**, 73–82.
- 15 A. J. W. G. Visser, J. S. Santema and A. van Hoek, Spectroscopic and dynamic characterization of FMN in reversed micelles entrapped water pools, *Photochem. Photobiol.*, 1984, **39**, 11–16.
- 16 A. J. W. G. Visser, K. Vos, J. S. Santema, J. Bouwstra and A. van Hoek, Static and time-resolved fluorescence of an amphiphilic flavin in Aerosol OT reversed micelles, *Photochem. Photobiol.*, 1987, **46**, 457–461.
- 17 *Reversed Micelles*, ed. P. L. Luisi and B. E. Straub, Plenum Press, New York, 1984.
- 18 A. Maitra, Determination of size parameters of water-Aerosol OT-oil reverse micelles from their nuclear magnetic resonance data, *J. Phys. Chem.*, 1984, **88**, 5122–5125.
- 19 M. Zulauf and H. F. Eicke, Inverted micelles and microemulsions in the ternary-system H₂O-Aerosol-OT-iso-octane as studied by photon correlation spectroscopy, *J. Phys. Chem.*, 1979, **83**, 480–486.
- 20 M. Wong, J. K. Thomas and T. Nowak, Structure and state of H₂O in reversed micelles. 3, *J. Am. Chem. Soc.*, 1977, **99**, 4730–4736.
- 21 J. Lang, A. Jada and A. Malliaris, Structure and dynamics of water-in-oil droplets stabilized by sodium bis(2-ethylhexyl) sulfosuccinate, *J. Phys. Chem.*, 1988, **92**, 1946–1953.
- 22 E. Keh and B. Valeur, Investigation of water-containing inverted micelles by fluorescence polarization – determination of size and internal fluidity, *J. Colloid Interface Sci.*, 1981, **79**, 465–478.
- 23 N. Wittouck, R. M. Negri, M. Ameloot and F. C. Deschryver, AOT reversed micelles investigated by fluorescence anisotropy of cresyl violet, *J. Am. Chem. Soc.*, 1994, **116**, 10601–10611.
- 24 P. E. Zinsli, Inhomogeneous interior of Aerosol OT microemulsions probed by fluorescence and polarization decay, *J. Phys. Chem.*, 1979, **83**, 3223–3231.
- 25 C. D. Borsarelli and S. E. Braslavsky, The nature of the water structure inside the pools of reverse micelles sensed by laser-induced optoacoustic spectroscopy (LLOAS), *J. Phys. Chem. B*, 1997, **101**, 6036–6042.
- 26 Z. L. Lai and P. Y. Wu, Investigation on the conformations of AOT in water-in-oil microemulsions using 2D-ATR-FTIR correlation spectroscopy, *J. Mol. Struct.*, 2008, **883**, 236–241.
- 27 J. H. Brannon and D. Magde, Absolute quantum yield determination by thermal blooming: fluorescein, *J. Phys. Chem.*, 1978, **82**, 705–709.
- 28 J. R. Lakowicz, *Principles of Fluorescence Spectroscopy*, Springer Science+Business Media, LLC, Singapore, 3rd edn, 2006.
- 29 A. S. R. Koti, M. M. G. Krishna and N. Periasamy, Time-resolved area-normalized emission spectroscopy (TRANES): a novel method for confirming emission from two excited states, *J. Phys. Chem. A*, 2001, **105**, 1767–1771.
- 30 L. Crovetto, V. Martinez-Junza and S. E. Braslavsky, Entropy changes drive the electron transfer reaction of triplet flavin mononucleotide from aromatic acids in cation-organized aqueous media. A laser induced optoacoustic study, *Photochem. Photobiol.*, 2006, **82**, 281–290.
- 31 T. B. Melø, M. A. Ionescu, G. W. Haggquist and K. R. Naqvi, Hydrogen abstraction by triplet flavins. I time-resolved multi-channel absorption spectra of flash-irradiated riboflavin solutions in water, *Spectrochim. Acta, Part A*, 1999, **55**, 2299–2307.
- 32 J. K. Eweg, F. Müller, A. J. W. G. Visser, C. Veeger, D. Bebelaar and J. D. W. van Voorst, Molecular luminescence of some isoalloxazines in apolar solvents at various temperatures, *Photochem. Photobiol.*, 1979, **30**, 463–471.
- 33 C. D. Borsarelli, J. J. Cosa and C. M. Previtali, Exciplex formation between pyrene derivatives and *N,N*-dimethylaniline in aerosol OT reversed micelles, *Langmuir*, 1992, **8**, 1070–1075.
- 34 E. Sikorska, I. V. Khmelinskii, D. R. Worrall, J. Koput and M. Sikorski, Spectroscopy and photophysics of iso- and alloxazines: experimental and theoretical study, *J. Fluoresc.*, 2004, **14**, 57–64.
- 35 S. Salzmann and C. M. Marian, Effects of protonation and deprotonation on the excitation energies of lumiflavin, *Chem. Phys. Lett.*, 2008, **463**, 400–404.
- 36 S. D. M. Islam, T. Susdorf, A. Penzkofer and P. Hegemann, Fluorescence quenching of flavin adenine dinucleotide in aqueous solution by pH dependent isomerisation and photo-induced electron transfer, *Chem. Phys.*, 2003, **295**, 137–149.
- 37 N. Mataga, Y. Kaifu and M. Koizumi, Solvent effects upon fluorescence spectra and the dipole moments of excited molecules, *Bull. Chem. Soc. Jpn.*, 1956, **29**, 465–470.
- 38 C. Reichardt, *Solvents and Solvent Effects in Organic Chemistry*, Wiley-VCH Verlag GmbH & Co. KGaA, Weinheim, 3rd edn, 2003.
- 39 A. J. W. G. Visser, K. Vos, A. van Hoek and J. S. Santema, Time-resolved fluorescence depolarization of rhodamine B and (octadecyl)rhodamine B in triton X-100 micelles and aerosol OT reversed micelles, *J. Phys. Chem.*, 1988, **92**, 759–765.
- 40 N. V. Shcherbatska, A. van Hoek, P. I. H. Bastiaens and A. J. W. G. Visser, Time-resolved fluorescence relaxation of 3-methylflavin in polar solution, *J. Fluoresc.*, 1995, **5**, 171–177.
- 41 C. D. Borsarelli, J. J. Cosa and C. M. Previtali, Photoinduced charge separation in reverse micelles prepared with benzylhexadecyldimethylammoniumchloride (BHDC). The electron-transfer reaction between pyrene and *N,N*-dimethylaniline, *Photochem. Photobiol.*, 1998, **68**, 438–446.
- 42 M. S. Altamirano, C. D. Borsarelli, J. J. Cosa and C. M. Previtali, Influence of polarity and viscosity of the micellar interface on the fluorescence quenching of pyrene compounds by indole derivatives in AOT reverse micelles solutions, *J. Colloid Interface Sci.*, 1998, **205**, 390–396.
- 43 A. J. W. G. Visser, Kinetic of stacking interactions in flavin adenine dinucleotide from time-resolved flavin fluorescence, *Photochem. Photobiol.*, 1984, **40**, 703–706.
- 44 G. F. Li and K. D. Glusac, The role of adenine in fast excited-state deactivation of FAD: a femtosecond mid-IR transient absorption study, *J. Phys. Chem. B*, 2009, **113**, 9059–9061.
- 45 S. Raffelberg, M. Mansurova, W. Gärtner and A. Losi, Modulation of the photocycle of a LOV domain photoreceptor by hydrogen-bonding network, *J. Am. Chem. Soc.*, 2011, **133**, 5346–5356.
- 46 A. Chattopadhyay, S. Mukherjee and H. Raghuraman, Reverse micellar organization and dynamics: a wavelength-selective fluorescence approach, *J. Phys. Chem. B*, 2002, **106**, 13002–13009.
- 47 M. Novaira, F. Moyano, M. A. Biasutti, J. J. Silber and N. M. Correa, An example of how to use AOT reverse micelle interfaces to control a photo-induced intramolecular charge-transfer process, *Langmuir*, 2008, **24**, 4637–4646.
- 48 P. A. W. van der Berg, J. Widengren, M. A. Hink, R. Rigler and A. J. W. G. Visser, Fluorescence correlation spectroscopy of flavins and flavoproteins: photochemical and photophysical aspects, *Spectrochim. Acta, Part A*, 2001, **57**, 2135–2144.
- 49 M. Green and G. Tollin, Flash photolysis of flavins. II. Quenching of the photoreactions, *Photochem. Photobiol.*, 1968, **7**, 145–153.
- 50 I. Ahmad and F. H. M. Vaid, in *Flavins: Photochemistry and Photobiology*, ed. E. Silva and A. M. Edwards, *Comprehensive series in Photochemistry and Photobiology – Vol 6*, Royal Society of Chemistry, 2006, ch. 2, pp. 13–40.
- 51 L. Valle and C. D. Borsarelli, *Photophysical Characterization of Flavins Cofactors in Organized Media*. XXVIII Argentinean Conference of Chemistry, National University of Lanús, Lanús, Argentina, September 13th–16th, 2010.